

(1963).

<sup>24</sup>E. H. Sondheimer and A. H. Wilson, Proc. Roy. Soc. (London) A203, 75 (1950).<sup>25</sup>P. L. Taylor, Proc. Phys. Soc. (London) A80, 755 (1962); Phys. Rev. 135, A1333 (1964).

PHYSICAL REVIEW B

VOLUME 6, NUMBER 10

15 NOVEMBER 1972

## Pseudopotential Calculations of the Electronic Structure of a Transition-Metal Compound—Niobium Nitride

C. Y. Fong

*Department of Physics, University of California, Davis, California 95616*

and

Marvin L. Cohen\*

*Department of Physics, University of California, and Inorganic Material Research Division, Lawrence Berkeley Laboratory, Berkeley, California 94720*

(Received 2 May 1972)

The electronic band structure, density of states, and  $\epsilon_2(\omega)$ , the imaginary part of the dielectric constant, are calculated for niobium nitride using the empirical-pseudopotential method. The results are compared with non-self-consistent and with the self-consistent augmented-plane-wave calculations. A discussion of the Fermi surface is included.

### I. INTRODUCTION

We have recently developed a scheme,<sup>1</sup> which is a simple modification of the usual form of the empirical-pseudopotential method<sup>2</sup> (EPM) for simple metals and semiconductors, to calculate the electronic properties of noble metals<sup>3</sup> and a transition metal—niobium.<sup>4</sup> The advantage of this scheme is its simplicity and its flexibility. In the case of the noble metals and the transition metal, this empirical scheme involves less (8) parameters than previous pseudopotential—tight-binding schemes. It is also unnecessary to know *a priori* the region in the Brillouin zone (BZ) where the hybridization between the *s* and *d* electrons is strongest for these crystals. All one needs are the energies at a few high-symmetry points inside the BZ and the width of the *d* bands. The energies and the width of the *d* bands can be determined by optical measurements<sup>3,5</sup> and photoemission experiments,<sup>6</sup> respectively. Furthermore, the atomic pseudopotential extracted from one calculation can be used at least as a starting potential for other compounds with the same atom as a constituent.<sup>2</sup> It is this flexibility which enables us to calculate the electronic properties of a series of compounds.

In this report we concentrate on a transition-metal compound. This class of compounds is extremely interesting. Some of these compounds are high-temperature superconductors, and others exhibit interesting metal-insulator transitions. It is felt that a vast amount of basic knowledge about solids can be obtained through studies of these

kinds of crystals, and it is, therefore, necessary to have an effective method to study the electronic properties of these compounds. We have anticipated in Ref. 1 that the EPM can be used for this purpose. Here, we report the first energy band structure of a transition-metal compound (niobium nitride) obtained by using the EPM. We would like to make a few comments about the significance of the present calculation: (a) Despite the fact that the band structure presented is fitted to first-principles calculations (due to the lack of experimental information) the results indicate that it is now possible to determine with even more accuracy the energy band structure of interesting transition-metal compounds if optical and photoemission data are available. (b) NbN is a high-temperature superconductor with  $T = 15.7^\circ\text{K}$ .<sup>7</sup> We anticipate that the pseudopotential derived here for NbN can be used in the future to study the origin of the high superconducting transition temperature for this compound. Furthermore, if more optical and photoemission data relating to the transition-metal compounds are available, one can use the results of the EPM to predict the superconducting transition temperature. (c) Experimental studies on NbN, up to present, are restricted to mechanical, electrical, and superconducting properties. If optical data were available we could refine our calculation. For the present, we give a calculation of the imaginary part of the dielectric function as a rough prediction of the optical spectrum. (d) Earlier theoretical studies were done by Mattheiss<sup>8</sup> (who also summarized results for similar compounds) using

the augmented-plane-wave (APW) method and by Schwarz<sup>9</sup> who used the self-consistent APW method. There exist large discrepancies between the two APW results. As we will show the results of the EPM fit Schwarz's calculations better than Mattheiss's results. This paper will be presented in four sections. In Sec. II, we discuss the method of calculation. The results are given in Sec. III. Finally, Sec. IV presents the summary and conclusions of this study.

## II. METHOD OF CALCULATION

The general form of the pseudopotential Hamiltonian has the following form:

$$\mathcal{H} = -\frac{\hbar^2}{2m} \nabla^2 + V_L(\vec{r}) + V_{NL}(\vec{r}), \quad (1)$$

where  $V_L(\vec{r})$  is the local pseudopotential and  $V_{NL}(\vec{r})$  is the nonlocal pseudopotential. The potential  $V_L(\vec{r})$  is expanded in the reciprocal lattice

$$V_L(\vec{r}) = \sum_{\vec{G}} V(|\vec{G}|) e^{i\vec{G} \cdot \vec{r}}, \quad (2)$$

where  $\vec{G}$  is a reciprocal-lattice vector in units of  $(2\pi/a)$ ,  $a$  is the lattice constant and is equal to  $4.39 \text{ \AA}$ .<sup>7</sup>  $V(|\vec{G}|)$  is the pseudopotential form factor. We truncate the series at  $|\vec{G}|^2 = 12$ . NbN has the rocksalt structure; the origin of the coordinate system is taken at the Nb atom and the position of N atom is at  $\frac{1}{2}a(1, 1, 1)$ . The truncation, then, leaves two antisymmetric form factors,  $V^A$ , at  $|\vec{G}|^2 = 3$  and  $11$  and three symmetric form factors,  $V^S$ , at  $|\vec{G}|^2 = 4, 8, \text{ and } 12$ .

$V_{NL}(\vec{r})$  contains two separate parts: (a) A  $d$ -wave nonlocal potential to account for the part of the potential for the  $d$  electrons of the Nb atom which is over canceled in  $V_L(\vec{r})$ . The form of this  $d$ -like  $V_{NL}(\vec{r})$ , centered at the Nb atom, is the same as given in Ref. 1 and has the following form:

$$V_{NL}^{l=2}(\vec{r}) = \sum_j P_2^\dagger V_2(|\vec{r} - \vec{R}_j|) P_2, \quad (3)$$

where  $\vec{R}_j$  is the lattice vector.  $P_2^\dagger$  and  $P_2$  are projection operators. They project out the  $l=2$  component of the wave functions when the matrix elements of the  $V_{NL}^{l=2}(\vec{r})$  are calculated over a convenient basis:

$$V_2(|\vec{r} - \vec{R}_j|) = A_2 \quad \text{for } |\vec{r} - \vec{R}_j| \leq R_2 \\ = 0 \quad \text{otherwise,} \quad (4)$$

where  $A_2$  and  $R_2$  are treated as disposable parameters. Since we want to obtain good convergence for the energy of the  $d$  band using a plane-wave basis, we introduce a damping factor of the form (as in Ref. 1):

$$\langle \vec{k} + \vec{G} | V_{NL}^{l=2}(\vec{r}) | \vec{k} + \vec{G}' \rangle$$

$$\rightarrow \exp - \alpha \left( \frac{1}{2k_F} (|\vec{k} + \vec{G}| - \kappa) \right)^2 \langle \vec{k} + \vec{G} | V_{NL}^{l=2}(\vec{r}) | \vec{k} + \vec{G}' \rangle \\ \times \exp \left[ - \alpha \left( \frac{1}{2k_F} (|\vec{k} + \vec{G}'| - \kappa) \right)^2 \right], \quad (5)$$

where  $\alpha$  and  $\kappa$  are treated as parameters and  $k_F$  is taken as the Fermi momentum of Nb.

(b) A  $p$ -wave nonlocal potential since the core states of the N atom is  $(1s)^2$  and there is no  $p$ -like core states. The valence states  $(2s)^2(2p)^3$  have both  $s$  and  $p$  characters. Similar to the case of boron nitride (BN)<sup>10</sup> we introduce a nonlocal pseudopotential for the  $p$  electrons. This  $p$ -like nonlocal pseudopotential takes the following form:

$$V_{NL}^{l=1}(\vec{r}) = \sum_j P_1^\dagger V_1(|\vec{r} - \vec{R}_j - \vec{\tau}|) P_1, \quad (6)$$

where  $P_1^\dagger$  and  $P_1$  are projection operators similar to  $P_2$  but they project out the  $l=1$  component only.  $\vec{R}_j$  is the same lattice vector defined above.  $\vec{\tau} = \frac{1}{2}a(1, 1, 1)$  so that  $V_1(\vec{r})$  is centered around the N atom in each unit cell:

$$V_1(|\vec{r}|) = A_1 r e^{-\beta r} \quad \text{for } |\vec{r}| \leq R_1 \\ = 0 \quad \text{otherwise,} \quad (7)$$

where  $A_1$  and  $\beta$  are treated as parameters. The value of  $R_1$  is set equal to the ionic radius<sup>11</sup>  $0.25 \text{ \AA}$  of  $N^+$ , it is not varied during the fitting process.

The pseudopotential Hamiltonian, then, is diagonalized over plane-wave basis states. In order to obtain convergence for the energies at  $\Gamma$ ,  $X$ , and  $L$  to within  $0.1 \text{ eV}$ , we use control energies<sup>1, 2, 12</sup>  $E_1 = 20.1$  and  $E_2 = 40.1$  in units of  $(2\pi/a)^2$ , the size of the matrix is of the order of  $100 \times 100$  and there are about 175 plane waves contributing to the Löwdin-Brust perturbation.<sup>12</sup>

## III. RESULTS

Because of the lack of optical and photoemission data for NbN, we decided to use the APW results to obtain values for the parameters in our theory. We started by extracting the N potential from BN.

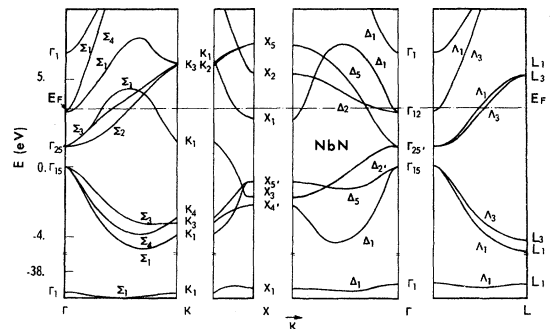


FIG. 1. Energy band structure of NbN.

TABLE I. Parameters for the pseudopotential for NbN.

Parameters for local pseudopotential	Parameters for nonlocal $d$ pseudopotential	Parameters for nonlocal $p$ pseudopotential
$V^A [ \vec{G} ^2 = 3(2\pi/a)^2] = 0.4442$ Ry	$R_s = 1.18$ Å	$R_1 = 0.25$ Å
$V^A(11) = 0.0600$	$\alpha = 0.118$	$\alpha = 1.15$ Å <sup>-1</sup>
$V^S(4) = -0.1812$	$\kappa = 1.73(2\pi/a)$	$A_1 = -0.67$ Ry/Å
$V^S(8) = -0.1411$	$A_2 = -4.8624$ Ry	
$V^S(12) = -0.0661$	$a = 4.39$ Å	

We then scaled both the extracted N potential and the Nb potential to the lattice constant of NbN. These scaled potentials are then adjusted to fit the energies obtained by the first-principles band calculations. We first tried to fit the results obtained by Mattheiss as we had done for Nb with the hope that a consistent Nb pseudopotential usable for both materials might be obtained. However, we obtained a reversal in the order of the  $L_3$  and  $L_1$  states for the valence bands. It was impossible to reverse this ordering without giving up the agreement for the energy gaps at  $\Gamma$  and X. We found that further variation gave results similar to the self-consistent APW results by Schwartz<sup>9</sup> and we then used this calculation to obtain our parameters. The ordering of the  $L_3$  and  $L_1$  states was still the main difficulty. We finally managed to obtain the same ordering as in Ref. 9, by sacrificing the agreement of the position of the  $X_1$  band derived from  $\Gamma_{12}$ . The resulting form factors and the parameters relating to the  $V_{NL}(\vec{r})$  are listed in Table I. We do not compare these values of the pseudopotential to the scaled ones for two reasons: (a) We obtained the Nb results using Mattheiss's<sup>8</sup>

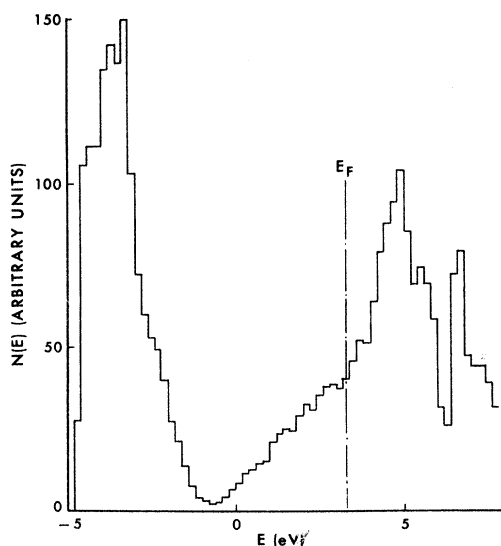


FIG. 2. Density of states of NbN.

results for pure Nb. In this calculation we use the results of Ref. 9, and the results between Refs. 8 and 9 are quite different. Therefore, we do not expect that the Nb potential from the present calculation will be consistent with the one obtained in Ref. 4 and without optical data we cannot decide which one is more accurate. (b) The scaled N potential from BN was not expected to be accurate, because only one piece of experimental information is used to determine the potential.

The band structure along various symmetry directions is given in Fig. 1. The best agreement between this calculation and the ones in Ref. 9 is for the  $\Gamma$  point of the BZ. A comparison of a few important energy gaps between the present results and Refs. 8 and 9 is given in Table II. The density of states derived from the band structure is plotted in Fig. 2. The Fermi energy is at 3.3 eV above

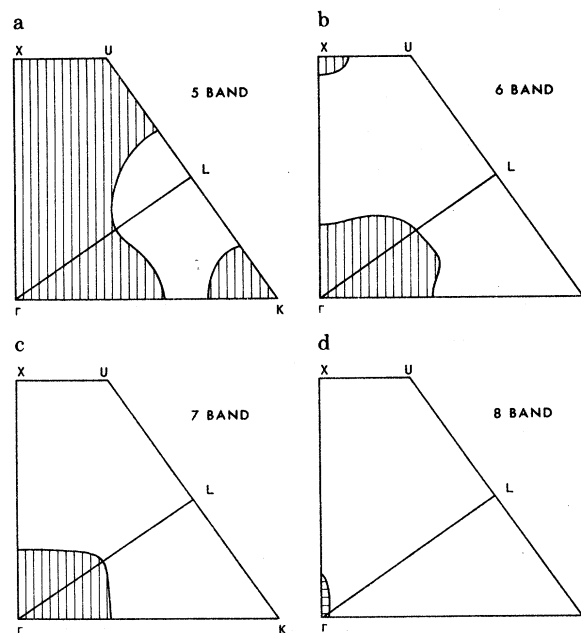


FIG. 3. (a) Shape of the Fermi surface for band 5; (b) shape of the Fermi surface for band 6; (c) shape of the Fermi surface for band 7; (d) shape of the Fermi surface for band 8.

TABLE II. Comparison of important energy gaps obtained from EPM and APW calculations.

Energy gaps Symmetry	Schwarz (APW self-consistent) eV	Mattheiss (APW) eV	Fong-Cohen (EPM) eV
$\Gamma_1 \rightarrow \Gamma_{15}$ (s-p)	6.54	9.67	6.52
$X_{4'} \rightarrow \Gamma_{15}$ (p-p)	2.39	1.2	2.25
$X_{5'} \rightarrow \Gamma_{15}$ (p-p)	0.6	0.38	0.9
$\Gamma_{15} \rightarrow \Gamma_{25'}$ (p-d)	1.14	5.24	1.14
$\Gamma_{15} \rightarrow \Gamma_{12}$	3.11	7.08	3.14
$L_1 \rightarrow \Gamma_{15}$	5.67	3.58	4.84
$L_3 \rightarrow \Gamma_{15}$	3.51	2.22	4.21
$X_3 \rightarrow \Gamma_{15}$	2.01	-2.27	1.74
$\Gamma_{15} \rightarrow X_1$	6.94	10.09	2.68

$\Gamma_{15}$ . The peak in the density of states for the lower bands is about 0.8 eV lower than the corresponding one in Ref. 9 measured with respect to  $\Gamma_{15}$ . This shows that our bands near  $K$  are lower in energy than the APW results. The peak of the density of states for the higher bands is at 4.9 eV above  $\Gamma_{15}$ . The APW results show a peak at 4.4 eV. The general shape and the relative magnitude of the peaks for both results agree quite well. The Fermi surface for bands 5, 6, 7, and 8 are given in Fig. 3. Band 9 is omitted because the Fermi surface for this band is a very small pocket centered around  $\Gamma$  (from the  $\Gamma_{12}$  level). Except for band 6, the shape of the bands is very similar to the ones in Ref. 9. For band 6, the bending of  $X_1$  gives a small pocket near  $X$ . One plausible reason for the bending of  $X_1$  is due to the hybridization. As we mentioned in Ref. 4, the pseudopotential results for Nb showed stronger hybridization than the APW results. Here, the hybridization is evident for the two  $\Delta_1$  bands, and it causes a lowering in energy of the band  $X_1$ . In order to provide some information about the optical properties of NbN and to stimulate experimental work, we give the joint density of states and  $\epsilon_2$ , the imaginary part of dielectric constant due to interband transitions only, with dipole matrix elements calculated by using pseudo-wave-functions in Figs. 3 and 4. The peak at 0.1 eV in both the joint density of states and  $\epsilon_2(\omega)$  is due to 6-7 transitions. However, the structure in  $\epsilon_2$  at 0.6 eV is from 5-6 transitions. This structure is caused by the matrix elements calculated in the pseudo-wave-functions approximation.

#### IV. CONCLUSION

We have presented preliminary results for NbN using the empirical-pseudopotential method. The energies were fitted to a self-consistent APW result by Schwarz.<sup>9</sup> The general agreement can be considered to be consistent to within approximately 0.5 eV. The main purpose of this calculation is to show that the empirical-pseudopotential method can now be applied to transition-metal compounds. In the future, when optical data become available,

systematic studies on these compounds can become feasible, and we expect that one can improve on the results presented here for NbN.

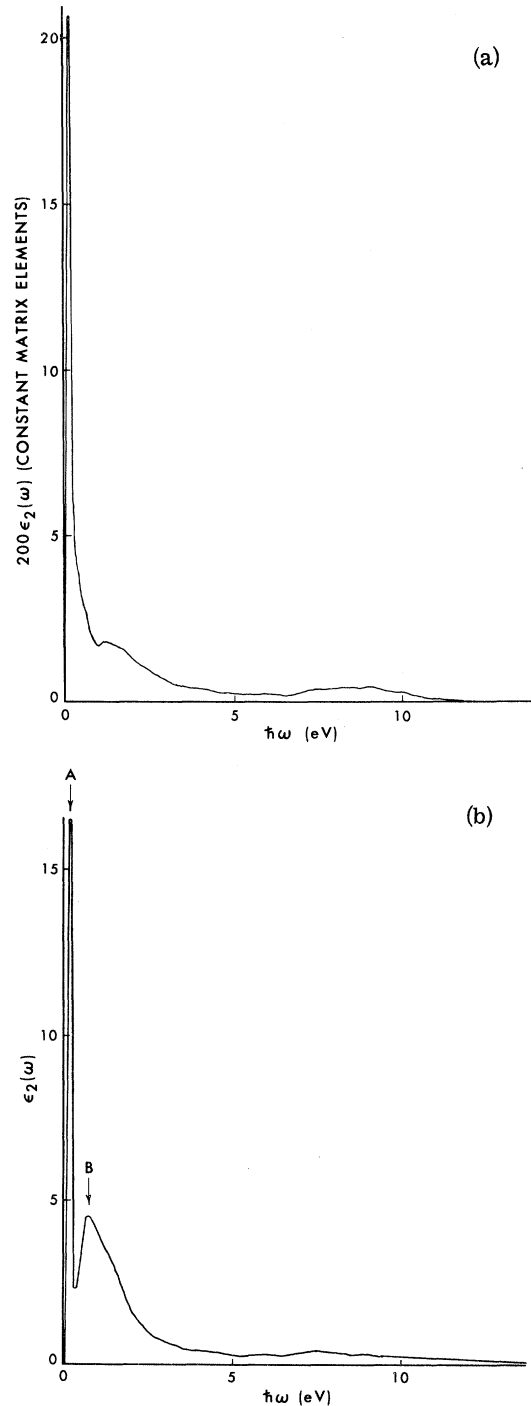


FIG. 4. (a) Joint density of states of NbN. (This is the same as the imaginary part of the dielectric function with constant matrix elements.) (b) The imaginary part of the dielectric function,  $\epsilon_2(\omega)$ , of NbN with dipole matrix elements calculated from pseudo-wave-functions.

## ACKNOWLEDGMENTS

We would like to thank Dr. L. F. Mattheiss for sending us his results before the publication and

several helpful conversations. Part of this work was done under the auspices of the U. S. Atomic Energy Commission.

\*Supported by the National Science Foundation under Grant No. GP 13632.

<sup>1</sup>C. Y. Fong and M. L. Cohen, *Phys. Rev. Letters* **24**, 306 (1970).

<sup>2</sup>M. L. Cohen and V. Heine, *Solid State Physics*, edited by F. Seitz and D. Turnbull (Academic, New York, 1970), Vol. 24, p. 37.

<sup>3</sup>C. Y. Fong, M. L. Cohen, R. R. L. Zucca, J. Stokes, and Y. R. Shen, *Phys. Rev. Letters* **25**, 1486 (1970); J. Stokes, Y. R. Shen, Y. W. Tsang, M. L. Cohen, and C. Y. Fong, *Phys. Letters* **38A**, 347 (1972).

<sup>4</sup>C. Y. Fong and M. L. Cohen, *Phys. Letters* (to be published).

<sup>5</sup>For example, U. Gerhardt, *Phys. Rev.* **172**, 651

(1968).

<sup>6</sup>For example, N. V. Smith, *Phys. Rev. B* **3**, 1862 (1971).

<sup>7</sup>T. H. Geballe, B. T. Matthias, J. P. Remeika, A. M. Clogston, V. B. Compton, J. P. Maita, and H. J. Williams, *Physics* **2**, 293 (1966).

<sup>8</sup>L. F. Mattheiss, *Phys. Rev. B* **5**, 315 (1972).

<sup>9</sup>K. Schwarz, *Monatsh. Chem.* **102**, 1400 (1972).

<sup>10</sup>L. A. Hemstreet, Jr. and C. Y. Fong, *Phys. Rev. B* **6**, 1464 (1972).

<sup>11</sup>L. Pauling, *The Nature of the Chemical Bond*, 3rd ed. (Cornell U. P., Ithaca, N. Y., 1960), p. 514.

<sup>12</sup>D. Brust, *Phys. Rev.* **134**, A1337 (1964).

## Calculation of the Cohesive Energies and Bulk Properties of the Alkali Metals\*

Frank W. Averill

*Quantum Theory Project, Williamson Hall, University of Florida, Gainesville, Florida 32601*

(Received 2 June 1972)

The cohesive energy and zero-pressure density of the alkali metals have been calculated using the self-consistent augmented-plane-wave method and the statistical ( $X\alpha$ ) exchange-correlation approximation. For the value of  $\alpha$  which makes a single determinant of atomic spin orbitals satisfy the virial theorem, the lighter alkali metals are computed to have cohesive energies and zero-pressure densities which are too large (errors of 22 and 16% for Li) with respect to experiment. To test the sensitivity of these results to the choice of  $\alpha$ , the same calculations have been performed with  $\alpha$  set equal to  $\frac{2}{3}$ . This choice of  $\alpha$  produced more uniformly good results for all the alkali metals with the largest errors occurring for cesium (errors of 7 and 9%, respectively). It is suggested that these results may be a consequence of the large change in the valence electronic charge density that occurs when the lighter alkali-metal atoms come together to form the solid. It is not suggested, however, that  $\alpha = \frac{2}{3}$  be used in all energy-band calculations.

### I. INTRODUCTION

In recent years an approximate method<sup>1</sup> (called the  $X\alpha$  method) has been developed for calculating the bulk properties of solids under pressure. The method is essentially one in which the exchange-correlation potential energy in a one-electron effective Schrödinger equation is approximated by a term proportional to the one-third power of the total electron charge density. The  $X\alpha$  approximation has already been applied to several solids with varying degrees of success,<sup>2-5</sup> but there is still a great deal of uncertainty both as to the accuracy and to the range of applicability of the method. It appeared that it would be informative to apply the  $X\alpha$  method to a whole family of closely related solids. Specifically, it was hoped that some understanding could be gained from the way the  $X\alpha$  meth-

od treated the various members of the family, and that perhaps some general over-all trends might be made manifest.

The obvious choice for such a family of solids is the alkali metals. Because of their relative simplicity, the alkali metals have long been a testing ground for new approximate methods in solid-state theory. Furthermore, there is now an abundance of experimental information<sup>6,7</sup> available on these metals.

### II. DESCRIPTION OF THE CALCULATION

In the  $X\alpha$  approximation, the total energy of a crystal may be written<sup>2,3,8,9</sup>

$$\langle E_{X\alpha} \rangle = \langle T_{X\alpha} \rangle + \langle U_{X\alpha} \rangle, \quad (1)$$

where  $\langle T_{X\alpha} \rangle$  is the total kinetic energy and  $\langle U_{X\alpha} \rangle$  is the total potential energy of the crystalline system.